Basic Study

Long-term effects of gestational diabetes mellitus on the pancreas of female mouse offspring

Enriqueta Muñoz-Islas, Edgar David Santiago-SanMartin, Eduardo Mendoza-Sánchez, Héctor Fabián Torres-Rodríguez, Laura Yanneth Ramírez-Quintanilla, Christopher Michael Peters, Juan Miguel Jiménez-Andrade

Enriqueta Muñoz-Islas, Edgar David Santiago-SanMartin, Eduardo Mendoza-Sánchez, Héctor Fabián Torres-Rodríguez, Laura Yanneth Ramírez-Quintanilla, Juan Miguel Jiménez-Andrade, Unidad Académica Multidisciplinaria Reynosa-Aztlán, Universidad Autónoma de Tamaulipas, Reynosa 88740, Tamaulipas, Mexico

Christopher Michael Peters, Department of Anesthesiology, Wake Forest University School of Medicine, Winston Salem, NC 27101, United States

Corresponding author: Juan Miguel Jiménez-Andrade, PhD, Professor, Unidad Académica Multidisciplinaria Reynosa-Aztlán, Universidad Autónoma de Tamaulipas, 16 Calle y Lago de Chapala, Col. Aztlán, Reynosa 88740, Tamaulipas, Mexico. jandrade@docentes.uat.edu.mx

Abstract

BACKGROUND
Prolonged fetal exposure to hyperglycemia may increase the risk of developing abnormal glucose metabolism and type-2 diabetes during childhood, adolescence, and adulthood; however, the mechanisms by which gestational diabetes mellitus (GDM) predisposes offspring to metabolic disorders remain unknown.

AIM
To quantify the nerve axons, macrophages, and vasculature in the pancreas from adult offspring born from mouse dams with GDM.

METHODS
GDM was induced by *i.p.* administration of streptozotocin (STZ) in ICR mouse dams. At 12 wk old, fasting blood glucose levels were determined in offspring. At 15 wk old, female offspring born from dams with and without GDM were sacrificed and pancreata were processed for immunohistochemistry. We quantified the density of sensory [calcitonin gene-related peptide (CGRP)] and tyrosine hydroxylase (TH) axons, blood vessels (endomucin), and macro-phages (CD68) in the splenic pancreas using confocal microscopy.

RESULTS
Offspring mice born from STZ-treated dams had similar body weight and blood glucose values compared to offspring born from vehicle-treated dams. However, the density of CGRP^{+} and TH^{+} axons, endomucin^{+} blood vessels, and CD68^{+} macrophages in the exocrine pancreas was significantly greater in offspring from

mothers with GDM *vs* control offspring. Likewise, the microvasculature in the islets was significantly greater, but not the number of macrophages within the islets of offspring born from dams with GDM compared to control mice.

CONCLUSION
GDM induces neuronal, vascular, and inflammatory changes in the pancreas of adult progeny, which may partially explain the higher propensity for offspring of mothers with GDM to develop metabolic diseases.

Key Words: Gestational diabetes mellitus; Immunohistochemistry; Confocal microscopy; Pancreas; Offspring

Core Tip: Gestational diabetes mellitus (GDM) predisposes offspring to develop metabolic disorders later in life, however, the underlying mechanisms are unknown. Here, using a well-established model of GDM, we report that while GDM did not modify body weight or blood glucose, it significantly increased the density of nerve axons, blood vessels, and macrophages in the pancreas of adult offspring born from dams with GDM.

INTRODUCTION

Gestational diabetes mellitus (GDM) is one of the most common complications associated with pregnancy and is defined as any degree of glucose intolerance that occurs with the onset or during pregnancy[1]. The prevalence of GDM has increased substantially in the last few decades, occurring in up to 25% of pregnancies in certain populations[2]. GDM not only results in negative effects on mothers but also on their offspring[1,3]. Epidemiological studies show long-term neurological, cardiovascular, and endocrinological complications in offspring[4-6]. Prolonged fetal exposure to hyperglycemia may increase the risk of developing abnormal glucose metabolism and type-2 diabetes (T2D) during childhood, adolescence, and adulthood[6-9]. However, the mechanisms that contribute to the development of metabolic disorders following maternal hyperglycemia remain elusive.

Recently, there has been considerable scientific interest in understanding the role of pancreatic innervation in regulating glucose metabolism[10]. Sympathetic and sensory nerve fibers innervate the exocrine and endocrine pancreas [11-14]. In experimental diabetes, increased sympathetic innervation of islets has been shown to convey inhibitory signals reducing insulin production and release[15,16]. Clinically, sympathetic hyperactivity precedes the development of diabetes in young non-obese Japanese[17] and Korean[18] adults. Similarly, sensory neuron innervation is also associated with the regulation of glucose metabolism in experimental diabetes. In rats with spontaneous non-insulin-dependent diabetes, there is an increased density of sensory nerve fibers innervating the pancreas that occurs before the development of hyperglycemia[19]. Furthermore, several studies demonstrate an inhibitory influence of sensory neuron-derived neuropeptides on insulin production and sensitivity[20,21].

Previous reports have shown that patients with T2D have increased density of blood vessels surrounding islets compared to healthy individuals[22]. Additionally, in rodent models of spontaneous diabetes, several cellular and vascular abnormalities occur in pancreatic tissue at pre-diabetic stages. Enhanced vascular endothelial growth factor (VEGF) levels have been reported to occur in β-cells leading to disorganized, hypervascularized, and fibrotic islets, progressive macrophage infiltration, and increased proinflammatory cytokine production[23,24]. Altogether, these findings suggest that pathological changes might occur in pancreatic tissue at prediabetic stages even prior to quantifiable hyperglycemia and/or insulin resistance.

Adult mouse offspring born from dams with GDM are more susceptible to developing metabolic disorders[25,26]; however, the underlying pathogenic mechanisms are not fully known. The current study aims to assess whether there are changes in the sensory and sympathetic innervation, vascularization, and macrophage infiltration in pancreatic tissue from adult mouse offspring born from dams with streptozotocin (STZ)-induced GDM.

MATERIALS AND METHODS

Animals
Male (*n* = 10) and female ICR (*n* = 20) mice were purchased from Bioinvert Laboratories (Mexico City, Mexico) at an age of 10-12 wk (body weight 20-25 g). They were given one week to acclimate before use. These animals were used for

mating and posterior female offspring mice and all of them were housed at a temperature of 22 °C ± 2 °C, maintained on a 12:12 h light/dark cycle, with free access to food and water following the Norma Oficial Mexicana NOM-062-ZOO-1999. All animal experiments were conducted following the national guidelines and the relevant national laws on the protection of animals. Efforts were made to minimize the number of animals used.

Gestational diabetes model

Mice were mated overnight, two or three females per male. The presence of a vaginal plug the next morning indicated gestation day 0.5 (GD 0.5). Gestational diabetes was induced by intraperitoneal administration of STZ (catalog number S0130; Sigma-Aldrich Co.) dissolved in sodium citrate buffer (pH: 4.5 0.1 M). The STZ was administrated for three consecutive days as follows: 100 mg/kg on gestational day 6.5, 100 mg/kg on gestational day 7.5, and 80 mg/kg on gestational day 8.5[27]. Other pregnant mice were administered sodium citrate buffer (pH: 4.5, 0.1 M) on the same days of gestation (vehicle group, VEH). Dams were randomly allocated to receive STZ or vehicle (Figure 1A). Dams treated with STZ were considered to experience GDM when glucose concentrations were higher than 11.1 mmol/L[28,29]. Based on this criterion, the GDM model was confirmed through the determination of blood glucose of the dams 48 h after the last STZ or VEH administration (at 10.5 d of gestation). The concentration of blood glucose through the caudal vein was measured (mmol/L; Accutrend Plus, Roche) following a 6-h fasting period (Figure 1A). In each offspring group, mice were born from at least 4 different dams. The offspring were weaned at 20-21 d old. Due to our previous study showing no differences in blood glucose concentrations and oral glucose tolerance test between male and female offspring at 14-16 wk old[30], only female offspring were used in this study.

### Tissue harvesting and immunohistochemistry

Female mice were humanely sacrificed at 15 wk of age, through deep anesthesia with a mixture of ketamine and xylazine (100/10 mg/kg) followed by transcardiac perfusion, first with phosphate-buffered saline (PBS, 0.01 M, pH: 7.4, 4 °C) and followed by 4% paraformaldehyde in PBS (Figure 1A). The pancreas was dissected from the peritoneal visceral, leaving the spleen and duodenum associated as anatomical reference[31]. Following dissection, tissue specimens were post-fixed for 24 h in the same fixative at 4 °C. Then, the tissue specimens were cryoprotected in 30% sucrose solution at 4 °C for at least 48 h before the tissue was processed for IHC. The pancreata were embedded in Tissue Plus® (catalog Fisher HealthCare, Houston, TX, United States) and cut on a cryostat (Leica CM1900, Leica Biosystems, II, United States) at a thickness of 40 µm in the frontal plane and mounted on glass microscope slides (Superfrost Plus, Fisher Scientific). The pancreatic sections were incubated for 12 h at room temperature with primary antibody against calcitonin gene-related peptide (CGRP, polyclonal rabbit anti-mouse 1:3000; Sigma Aldrich; catalog number C8198) to label primary afferent sensory peptidergic nerve fibers. Sympathetic nerve fibers were labeled with primary antibody against tyrosine hydroxylase (TH, polyclonal rabbit anti-mouse 1:1000; EMD Millipore; catalog number AB152). An anti-endomucin (monoclonal rat anti-mouse 1:500; Santa Cruz; Catalog Number SC-65495) antibody was used for blood vessels. For activated macrophages, an antibody against CD68 primary antibody (Macrosialin; monoclonal rat anti-mouse 1:3000; Bio-Rad; catalog number MCA1957) was employed. Subsequently, preparations were washed in PBS and then incubated for 3 h with the secondary antibody (Cy3 monoclonal donkey anti-rabbit 1:600; Jackson ImmunoResearch; Catalog number 711-165-152 and Cy2 monoclonal donkey anti-rat 1:300; Jackson ImmunoResearch; Catalog number 712-225-150). Then, pancreatic sections were washed in PBS, dehydrated through an alcohol gradient (70%, 80%, 90%, and 100%), cleared in xylene, and coverslipped with a DPX mounting medium. Nuclear stain 4,6-diamidino-2-phenylindole (DAPI; 1:20000; Invitrogen; catalog number D21490) was used to visualize all cell nuclei.

Quantification of the density of nerve fibers, blood vessels, and macrophages

Previous studies have shown that the density of islets of Langerhans[32], as well as the density of sympathetic nerve fibers[31], is not significantly different between the duodenal and splenic pancreatic regions. Thus, in the present study, we determined the density of nerve fibers, blood vessels, and macrophages only in the splenic pancreas (Figure 1D). For this purpose, approximately 12 separate 40-µm-thick frozen sections were obtained from the pancreas of each mouse. To quantify nerve fibers (CGRP and TH), one image per section was acquired within the acinar tissue in the splenic pancreas through a Carl Zeiss scanning confocal laser microscope (Model LSM 800, Jena Germany) using a 20x air, scan zoom 2.0 objective. Then, images were analyzed using ImageJ software (National Institutes of Health) and nerve fibers were manually traced by a blinded investigator, using the freehand line tool, to determine the total length of nerve fibers. Data from at least three sections per mouse (separated by at least 100 µm) from the splenic pancreas were recorded and averaged. The total volume was calculated by tracing the area of the image and multiplying it by the thickness of the section (40 µm). The signal/noise ratio for nerve profiles within the islets was very low which did not allow us to obtain reliable quantification. Therefore, the density of nerve fibers was performed only in the exocrine pancreas. Data were expressed as the total length of nerve fibers per volume of the acinar pancreatic tissue (mm/mm^3).

The quantification of the density of CD68-immunoreactive cells in pancreatic tissue was adapted from previous studies [33-35]. After IHC staining, three confocal images were acquired with a 20x air objective (aperture of 0.5; scan zoom 2.0 ×). Areas with greater CD68$^+$ expression were identified in the acinar cells or the islets of Langerhans of the splenic pancreas located 3 mm away from the spleen. Quantification was performed by visualizing all focal planes of the Z-axis counting as positive those CD68$^+$ profiles having one DAPI-stained nucleus. The number of cells was calculated in 1mm^3 of volume. For pancreas islets, it was considered the area of the islet.

The quantification of the density of endomucin-immunoreactive blood vessels was made both in acinar cells and islets of Langerhans (Figure 1D). One image per section was acquired within the acinar cells in the splenic pancreas with an epifluorescence microscope (Axio Scope.A1, Carl Zeiss, Jena, Germany; 20x), or in the islets of the pancreas with a
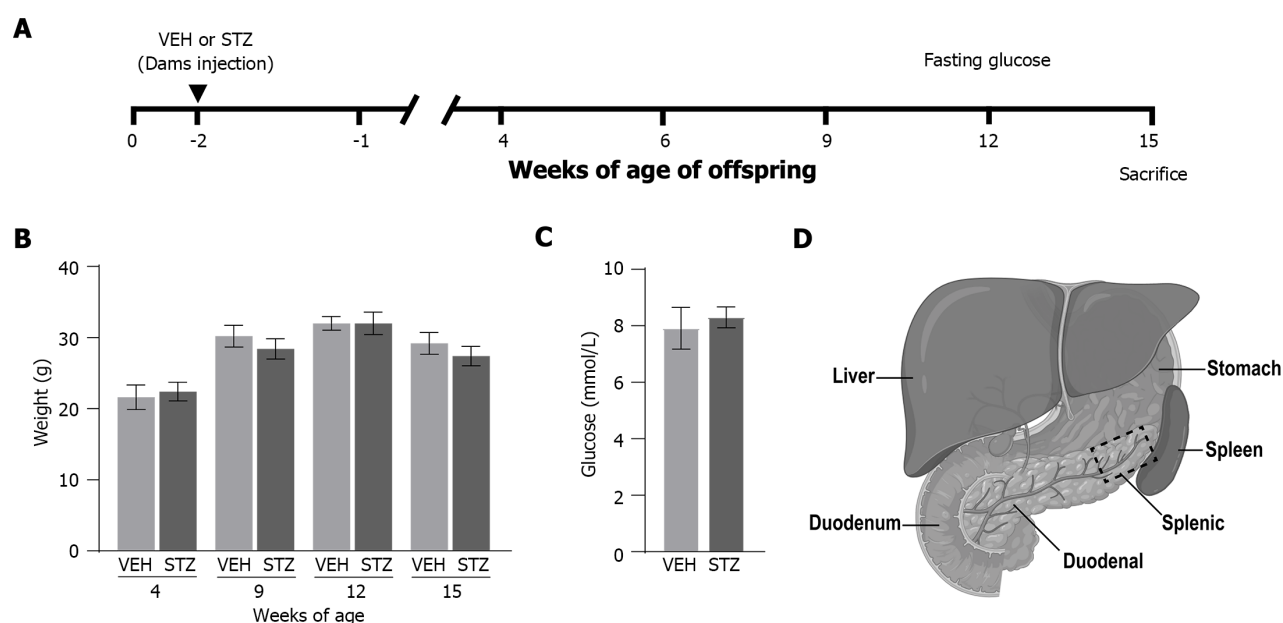
Figure 1 Experimental design, body weight, and blood glucose levels of female offspring born from control dams or dams with gestational diabetes mellitus. A: Diagram showing the experimental design and timeline; B and C: Female offspring born from dams treated with streptozotocin during pregnancy did not show significant changes in body weight or blood glucose compared to offspring born from dams treated with vehicle as controls; D: Scheme showing the region selected for quantification (splenic pancreas; square) of the neuronal, vascular, and inflammatory changes using immunohistochemistry and confocal microscopy. Data are shown as mean ± SEM, *n* = 5 per group. STZ: Streptozotocin; VEH: Vehicle.

confocal microscope. The number of blood vessels was determined in three different sections of the splenic pancreas. A blood vessel was counted only when it had a diameter between 2-10 μm[35]. The results were expressed as the mean number of blood vessels per area of interest (mm²). The area was obtained for acinar cells tracing the image, and for islets, it was adjusted per total islet area.

Immunohistochemistry on whole pancreatic tissue

This clearing method was adapted from a previous study[36]. Briefly, intestines and mesenteric fat tissues were carefully dissected at the level of the pancreas and duodenum. Intestines were flushed with PBS 0.01 M using a 23G syringe to remove fecal content. The tissues were fixed with 4% paraformaldehyde at 4 °C for 24 h and then washed with PBS 0.01 M three times for 1 h each. The samples were dehydrated with gradients of ethanol (20%, 40%, 60%, and 80%) and then incubated at 4 °C overnight with a solution of 30% H_2O_2 and 100% ethanol (1:10) to decolorize. The tissues were rehydrated through reverse ethanol gradients for 30 min each (100%, 80%, 60%, 40%, and 20%) and 0.01M PBS for 1 h twice. The samples were permeabilized with a solution containing 0.2% Triton X-100 (Sigma Aldrich, Catalog Number X-100), 0.1% Deoxycholate sodium (Sigma Aldrich, Catalog Number D6750-25G), 10% DMSO (Fisher Bioreagents, Catalog Number BP231-1), in 0.01 M PBS (solution pH: 6.5) and incubated for 72 h at 37 °C. Subsequently, the samples were blocked with 0.2% Triton X-100/10% DMSO/5% Normal Donkey Serum/10 mg/mL heparin (Sigma Aldrich, Catalog Number H3393-100KU) in 0.01M PBS solution for 24 h (solution pH: 6.5). Then the samples were stained with primary antibody against endomucin and secondary antibody (Cy3 monoclonal donkey anti-rat 1:600) for 72 h each at room temperature. Later, whole pancreatic tissue was washed with 0.01 M PBS and dehydrated with gradients of ethanol. Finally, the samples were mounted in the histology chamber, and cleared in dibenzyl ether (Sigma Aldrich; Catalog number 108014-1KG). Three-dimensional imaging of islets of Langerhans was obtained using a ZEISS LSM 800 confocal microscope with a 20x air objective. Imaris Viewer Version 10.0.1 software package for Windows (Oxford Instruments Inc.) was used to generate 3D images.

Statistical analysis

Data were represented as the mean ± SEM of groups of 5 mice each. Either a student *t*-test or two-way repeated measures ANOVA followed by a Tukey *post hoc* test was run when appropriate. Statistical significance was accepted at *P* < 0.05. All statistical analyses were performed using GraphPad Prism version 8.0 software package for Windows (GraphPad Software Inc., San Diego, CA, United States).

RESULTS

Effects of STZ-induced GDM on blood glucose levels and body weight of adult mice offspring

The administration of STZ in dams resulted in fasting blood glucose levels of (13.26 mmol/L ± 1.18 mmol/L), which were
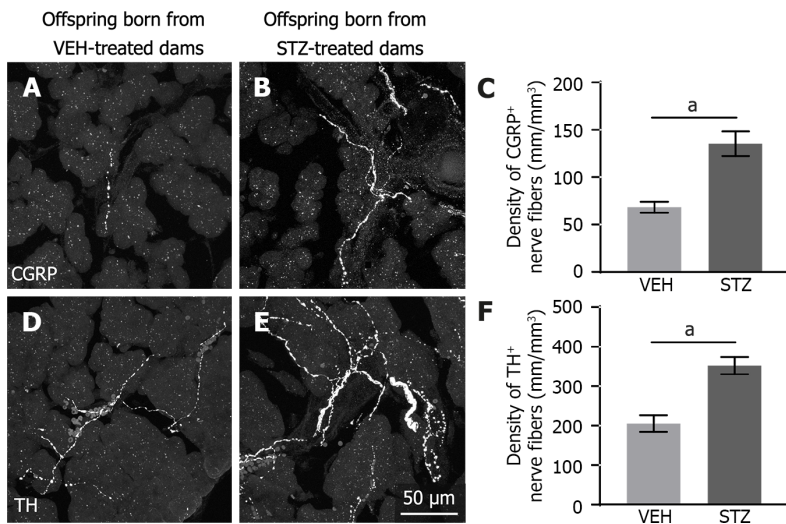
Figure 2 Adult female offspring born from dams with streptozotocin-induced gestational diabetes mellitus have increased density of sensory and sympathetic nerve fibers innervating the pancreatic acinar cells. A and B: Representative confocal images of calcitonin gene-related peptide (CGRP) expressing small diameter peptidergic sensory nerve fibers; C and F: Significantly greater densities of CGRP$^+$ and tyrosine hydroxylase$^+$ (TH$^+$) nerve fibers were found in offspring born from dams with GMD as compared to control offspring; D and E: Enzyme TH expressing postganglionic sympathetic nerve fibers in acinar pancreatic tissue (40 μm-thick) from offspring born of vehicle or streptozotocin injected dams; $^a P < 0.05$ Student *t* test, *n* = 5 per group. Data are shown as mean ± SEM. CGRP: Calcitonin gene-related peptide; TH: Tyrosine hydroxylase; VEH: Vehicle; STZ: Streptozotocin.

significantly higher as compared to those dams treated with vehicle (9.57 mmol/L ± 0.26 mmol/L). To determine the influence of GDM on the development of offspring, body weight was registered every week, and fasting blood glucose levels were determined at week 12 of age (Figure 1A). There were no significant changes in body weight (Figure 1B) or blood glucose levels (Figure 1C) of offspring born from dams treated with STZ compared to offspring born from dams treated with vehicle.

STZ-induced GDM increased the density of sensory and sympathetic nerve fibers innervating the acinar pancreatic tissue from adult female offspring

Sensory and sympathetic nerve fibers innervating the acinar cells from the splenic pancreas were detected using CGRP and TH antibodies, respectively. Representative confocal images show CGRP- (Figure 2A and B) and TH- (Figure 2D and E) immunoreactive nerve fibers present along the acinar cells. CGRP nerve fibers (Figure 2A) were less prominent than TH nerve fibers (Figure 2D) in control tissue. However, exocrine pancreatic tissue from adult offspring born from mice treated with STZ showed a significantly greater innervation of sensory CGRP (Figure 2B and C), and sympathetic TH (Figure 2E and F) fibers as compared to control mice (Figure 2A and D).

GDM increases blood vessel density both in acinar cells and islets of Langerhans

Endomucin-positive blood vessels were distributed throughout acinar tissue and had a tortuous appearance (Figure 3A and B). Quantitative analysis using confocal images showed that the density of blood vessels in offspring born from dams treated with STZ (Figure 3B and C) was significantly higher compared with offspring treated with vehicle (Figure 3A).

Endomucin immunoreactivity showed blood vessels well distributed through the pancreatic islet. These endomucin$^+$ blood vessels had a tortuous form. They were in a greater number in the tissue of offspring born from STZ-treated dams (Figure 3E) as compared to the control group (Figure 3D). The quantitative analysis revealed that GDM induced a significant increase in the number of blood vessels per total islet area in offspring from GDM dams as compared with offspring from dams treated with vehicle (Figure 3F). The islet area in offspring born from control dams was 124284.25 μm^2 ± 992.40 μm^2 and this tends to decrease to 91431.23 μm^2 ± 1382.00 μm^2 in progeny from dams with STZ-induced GDM (*P* = 0.355; unpaired *t*-test). Additionally, a solvent-based clearing method from whole pancreatic tissue was used to visualize the distribution of the blood vessels in an intact whole islet of Langerhans. Three-dimensional imaging of the islet showed increased intra-islet vasculature in offspring from GDM dams *vs* offspring from control dams (Figure 3G and H).

STZ-induced GDM increased the density of macrophages in the exocrine, but not the endocrine pancreatic tissue of adult female offspring

Immunohistochemical and confocal analysis revealed that macrophages are uniformly distributed in the acinar cells and pancreatic islets. In the acinar cells, the CD68$^+$ macrophages in the control tissue (Figure 4A) had a smaller size compared to those in the pancreatic tissue of adult offspring born from dams with GDM (Figure 4B). Macrophages in the acinar cells of GDM offspring also had a hypertrophied multivacuolated appearance indicative of active phagocytic macrophages (Figure 4B). GDM induced a statistically significant increase in the number of macrophages in the acinar pancreatic tissue of the offspring as compared to the control group (Figure 4C). On the other hand, quantitative analysis using confocal
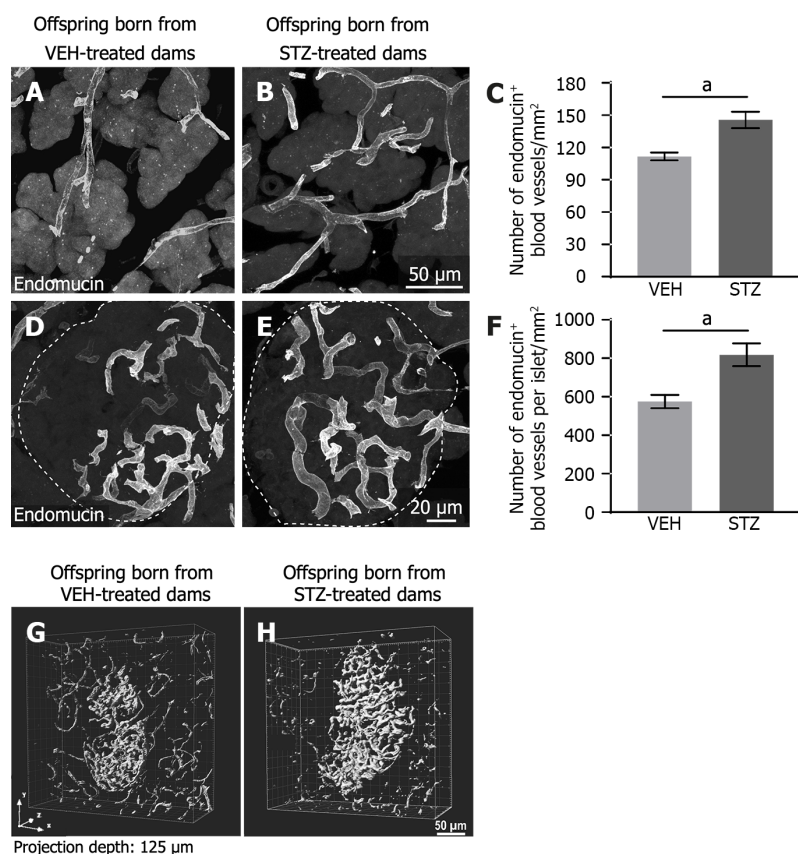
Figure 3 Adult female offspring born from dams with streptozotocin-induced gestational diabetes mellitus have a greater density of blood vessels vascularizing the acinar cells and the pancreatic islets. A, B, D and E: Representative confocal images of vehicle showing the endocrine and exocrine pancreatic tissue immunostained for endomucin blood vessels from adult progeny born from dams treated with vehicle or streptozotocin (STZ); C and F: There was a significantly greater density of blood vessels positive to endomucin in the acinar cells and the islets of Langerhans of offspring mice born from mice treated with STZ as compared to control mice; G and H: 3D visualization of the islet of Langerhans from whole pancreatic tissue processed with a solvent-based clearing method. Three-dimensional images of a cleared pancreas show an increased intra-islet vasculature. $^{a}P < 0.05$ Student *t* test, *n* = 4-5 per group. Data are shown as mean ± SEM. VEH: Vehicle; STZ: Streptozotocin.

images shows that macrophages in the pancreatic islets were distributed at the same proportions in the control group (Figure 4D and F) compared to the STZ group (Figure 4E).

DISCUSSION

This study reports for the first time that while adult offspring born from STZ-induced GDM do not exhibit alterations in body weight and glucose levels as compared to their age-matched respective controls[30], they have significant alterations at a cellular level in their pancreas. These include an increased density of a subset of sensory and sympathetic nerve fibers innervating exocrine pancreatic tissue along with an enhanced vasculature and macrophage infiltration in the exocrine pancreas. It was also found that there is an increased vasculature within the islets in these adult offspring exposed to GDM.

Both in the present study and in our previous report[30], we found that levels of blood glucose and glucose tolerance in adult mouse offspring (15 wk old) were not significantly impaired. Accordingly, adult mouse offspring born from dams with STZ-induced GDM at 3-6 months of age had normal blood glucose levels and did not exhibit any glucose intolerance [37]. However, it is possible to hypothesize that GDM-induced fetal hyperglycemia could program the body to respond differently to metabolic challenges later in life, increasing the susceptibility to develop metabolic alterations and dysfunction in glucose metabolism when they are older. In support of this, a recent study showed that while mice offspring born from dams with GDM are normoglycemic, they are more susceptible to becoming glucose intolerant when they are exposed to a short period of a high-fat diet[25]. Additionally, mouse offspring born from STZ-induced GDM dams develop both impaired glucose tolerance and decreased insulin sensitivity when they are 40 wk, but not, at 12 wk old[26].

It has been reported that the risk of prediabetes/diabetes in the offspring of mothers with GDM is eight times greater compared to offspring from mothers without GDM[6-9]. Given that the risk of developing T2D is greater in individuals whose mothers were diabetic when they were in utero as compared with offspring born from diabetic fathers and siblings born before the onset of maternal diabetes, it has been proposed that these long-term consequences of altered glucose

Offspring born from
VEH-treated dams

Offspring born from
STZ-treated dams
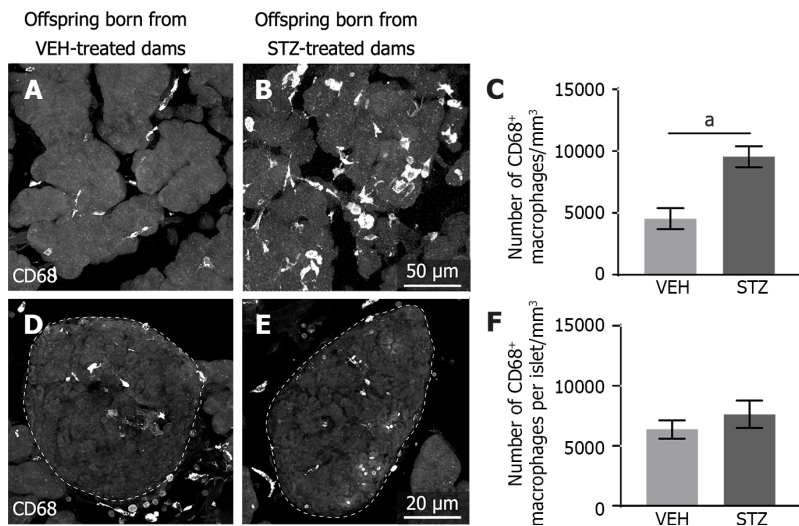
Figure 4 Adult female offspring born from dams with streptozotocin-induced gestational diabetes mellitus have an increased number of macrophages in the pancreatic acinar cells, but not in the pancreatic islets. A, B, D, and E: Representative confocal images of pancreatic cells expressing CD68 (cluster of differentiation 68) for macrophage staining in acinar pancreatic tissue or pancreatic islets from offspring born of vehicle or streptozotocin (STZ) injected dams (40 μm-thick); C and F: Significantly greater number of macrophages were found in the acinar pancreatic tissue, but not in the pancreatic islets of offspring born from dams treated with STZ compared to control mice. $^aP < 0.05$ Student t test, n = 4-5 per group. Data are shown as mean ± SEM. CD68: Cluster of differentiation 68; VEH: Vehicle; STZ: Streptozotocin.

metabolism result mainly from the fetal environment in GDM[38]. Intrauterine exposure to hyperglycemia may generate an *in-utero* environment around the fetus which programs them to disease during adulthood. This phenomenon has been recently called "*metabolic memory*"[39]. However, the specific underlying mechanisms by which fetal exposure to hyperglycemia may affect fetal development and impair glucose metabolism in the offspring are not fully known. It was recently demonstrated that adult mouse offspring born from STZ-induced GDM have dyslipidemia, insulin resistance, and glucose intolerance with advanced age (at 40 and 70, but not at 12 wk). Additionally, metabolic dysfunction and alterations in patterns of DNA methylation of genes involved in regulating glucose metabolism have also been reported [26]. Consistent with these studies, we also report in the current study GMD-induced long-term abnormalities and pathological changes in the pancreatic tissue of mouse offspring.

An increased density of TH nerve fibers in the exocrine pancreas has been reported in mice that spontaneously develop T2D[15] and in patients with T2D[10]. Moreover, the density of these sympathetic nerve fibers in pancreatic tissue parallel worsening glucose tolerance[10]. Finally, it has been shown that sympathetic nerve hyperactivity precedes hyperinsulinemia in young nonobese Japanese individuals[17], and a deviation in sympathovagal imbalance to sympathetic activity precedes the development of diabetes in young Korean adults[18]. Regarding CGRP nerve fibers, both exocrine and endocrine pancreata from mice[31] and different mammals including humans[40] are highly innervated by this subtype of sensory nerve fiber. Chemical ablation of CGRP nerve fibers prevents glucose homeostasis deterioration through increased insulin secretion in Zucker diabetic rats, an animal model for some aspects of human T2D[41].

Furthermore, a significant increase in the length of CGRP nerve fibers innervating pancreatic tissue from Otsuka Long-Evans Tokushima fatty rats (a model of human non-insulin-dependent diabetes) at 16 wk old was previously reported, even though they did not have increased fasting plasma glucose levels[19]. Preclinical and clinical evidence has also shown an increased vascularization, altered microvasculature, and macrophage infiltration in pancreatic tissue, and it has been proposed that these anatomical changes may contribute to a deterioration of -cell/islet function and exacerbate -cell loss in T2D[22,42-44]. Furthermore, an increased number of macrophages are detectable very early in islets, before the onset of diabetes in both high-fat-fed mice and Goto-Kakizaki rats[44]. Although we did not evaluate whether these neuroanatomical and cellular changes in the mouse pancreas from adult offspring are directly associated with a greater predisposition to develop T2D and/or another metabolic disease, the above studies support our hypothesis that these pathological changes may precede the development of metabolic diseases.

Our study demonstrates that an uncontrolled hyperglycemic state during pregnancy induces long-term alterations in pancreatic tissue from adult mouse offspring born from dams with GDM. While the mechanisms behind these GDM-induced long-term complications are unknown, based on the literature we propose these hypotheses. First, the alterations found in the pancreatic tissue from adult offspring could be due to direct toxic effects induced by STZ in the developing embryos since it was injected *i.p.* at the seventh day of gestation. However, cell death in fetuses from dams treated with STZ is similar in magnitude compared to that found in fetuses from dams treated with vehicle[45]. Additionally, while STZ can cross the placenta, it has a very short half-life (7 min). Based on this, it is unlikely that the alterations found result from a direct effect of STZ on the earliest stages of embryonic development[46]. Second, an increased density of sympathetic and sensory nerve fibers could be related to chronic hyperglycemia-induced alterations in the expression/function of neurotrophins and their receptors during fetal growth, which are pivotal for neuronal growth, differentiation, and survival of neurons innervating visceral organs including the pancreas[47,48]. As well as, increased vascularization and macrophage infiltration could result from impaired synthesis of key molecules regulating cell growth, vasculo-

genesis, and angiogenesis. Accordingly, endothelial nitric oxide synthase and *VEGF* genes are increased in embryos from mouse dams with STZ-induced GDM[49].

The present study has some limitations. First, we recognize that while we found cellular alterations in the pancreatic tissue from adult offspring born from dams with GDM, there is a need to assess whether these anatomical changes are translated into functional alterations such as a higher propensity to develop and/or greater severity of metabolic disease. Secondly, it is not possible to discern whether the increase in endomucin+ blood vessels[50] will result in changes in pancreatic blood flow. Third, while we observed an increase in the number of macrophages around acinar cells of offspring of GDM dams; it is unknown whether this macrophage infiltration will lead to altered production of pro-inflammatory and/or anti-inflammatory cytokines. Finally, we do recognize that these anatomical alterations were found at one time-point in life, however, it is warranted to determine when these changes start and/or to assess whether they disappear with aging.

CONCLUSION

We found a significant increase in the density of CGRP+ sensory and TH+ sympathetic axons, as well as a greater vascularization and macrophage infiltration in the exocrine pancreas and an increase in the number of blood vessels in pancreatic islets of female adult offspring born from dams with STZ-induced GDM, but without increased fasting blood glucose levels. Understanding the factors driving this neuroplasticity and cellular/vascular alterations may provide pharmacologic insight and targets for controlling these long-term metabolic complications of GDM in adult progeny.

ARTICLE HIGHLIGHTS

Research background
Epidemiological studies have shown several long-term neurological, cardiovascular, and endocrinological complications of gestational diabetes mellitus (GDM) in offspring.

Research motivation
Although there are several reports about the metabolic long-term complications of GDM on offspring, there is scarce information about the pathological changes at a cellular level that occur in the pancreas of offspring born from dams with GDM.

Research objectives
To quantify a subset of sensory and sympathetic nerve fibers, macrophages, and vasculature in the pancreas from adult offspring born from mouse dams with GDM.

Research methods
GDM was induced by *i.p.* administration of streptozotocin (STZ) in ICR mouse dams. Adult female offspring born from dams with and without GDM were sacrificed and pancreata were processed for immunohistochemistry. There was a quantification of the density of sensory (CGRP) and sympathetic (TH) axons, blood vessels (endomucin), and macrophages (CD68) in the splenic pancreas using confocal microscopy.

Research results
Offspring mice born from STZ-treated dams had similar body weight and blood glucose values compared to offspring born from vehicle-treated dams. However, the density of CGRP+ and TH+ axons, endomucin+ blood vessels, and CD68+ macrophages in the exocrine pancreas was significantly greater in offspring from mothers with GDM *vs* control offspring. Likewise, the microvasculature in the islets was significantly greater, but not the number of macrophages within the islets of offspring born from dams with GDM compared to control mice.

Research conclusions
GDM induces neuronal, vascular, and inflammatory changes in the pancreas of adult progeny, which may partially explain the higher propensity for offspring of mothers with GDM to develop metabolic diseases.

Research perspectives
Future studies are needed to evaluate the functional implications of these alterations and determine if their blockade with mechanism-based therapies may decrease the risk of developing impaired glucose tolerance and type-2 diabetes in individuals born from women with GDM.

FOOTNOTES

REFERENCES

1   **Buchanan TA**, Xiang AH, Page KA. Gestational diabetes mellitus: risks and management during and after pregnancy. *Nat Rev Endocrinol* 2012; **8**: 639-649 [PMID: 22751341 DOI: 10.1038/nrendo.2012.96]

2   **American Diabetes Association Professional Practice Committee**. 15. Management of Diabetes in Pregnancy: Standards of Medical Care in Diabetes-2022. *Diabetes Care* 2022; **45**: S232-S243 [PMID: 34964864 DOI: 10.2337/dc22-S015]

3   **Crowther CA**, Hiller JE, Moss JR, McPhee AJ, Jeffries WS, Robinson JS; Australian Carbohydrate Intolerance Study in Pregnant Women (ACHOIS) Trial Group. Effect of treatment of gestational diabetes mellitus on pregnancy outcomes. *N Engl J Med* 2005; **352**: 2477-2486 [PMID: 15951574 DOI: 10.1056/NEJMoa042973]

4   **Márquez-Valadez B**, Valle-Bautista R, García-López G, Díaz NF, Molina-Hernández A. Maternal Diabetes and Fetal Programming Toward Neurological Diseases: Beyond Neural Tube Defects. *Front Endocrinol (Lausanne)* 2018; **9**: 664 [PMID: 30483218 DOI: 10.3389/fendo.2018.00664]

5   **Pathirana MM**, Lassi ZS, Roberts CT, Andraweera PH. Cardiovascular risk factors in offspring exposed to gestational diabetes mellitus in utero: systematic review and meta-analysis. *J Dev Orig Health Dis* 2020; **11**: 599-616 [PMID: 31902382 DOI: 10.1017/S2040174419000850]

6   **Bianco ME**, Josefson JL. Hyperglycemia During Pregnancy and Long-Term Offspring Outcomes. *Curr Diab Rep* 2019; **19**: 143 [PMID: 31754898 DOI: 10.1007/s11892-019-1267-6]

7   **Scholtens DM**, Kuang A, Lowe LP, Hamilton J, Lawrence JM, Lebenthal Y, Brickman WJ, Clayton P, Ma RC, McCance D, Tam WH, Catalano PM, Linder B, Dyer AR, Lowe WL Jr, Metzger BE; HAPO Follow-up Study Cooperative Research Group; HAPO Follow-Up Study Cooperative Research Group. Hyperglycemia and Adverse Pregnancy Outcome Follow-up Study (HAPO FUS): Maternal Glycemia and Childhood Glucose Metabolism. *Diabetes Care* 2019; **42**: 381-392 [PMID: 30617141 DOI: 10.2337/dc18-2021]

8   **Saravanan P**; Diabetes in Pregnancy Working Group; Maternal Medicine Clinical Study Group; Royal College of Obstetricians and Gynaecologists, UK. Gestational diabetes: opportunities for improving maternal and child health. *Lancet Diabetes Endocrinol* 2020; **8**: 793-800 [PMID: 32822601 DOI: 10.1016/S2213-8587(20)30161-3]

9   **Dabelea D**, Hanson RL, Lindsay RS, Pettitt DJ, Imperatore G, Gabir MM, Roumain J, Bennett PH, Knowler WC. Intrauterine exposure to diabetes conveys risks for type 2 diabetes and obesity: a study of discordant sibships. *Diabetes* 2000; **49**: 2208-2211 [PMID: 11118027 DOI: 10.2337/diabetes.49.12.2208]

10 **Cinti F**, Mezza T, Severi I, Suleiman M, Cefalo CMA, Sorice GP, Moffa S, Impronta F, Quero G, Alfieri S, Mari A, Pontecorvi A, Marselli L, Cinti S, Marchetti P, Giaccari A. Noradrenergic fibers are associated with beta-cell dedifferentiation and impaired beta-cell function in humans. *Metabolism* 2021; **114**: 154414 [PMID: 33129839 DOI: 10.1016/j.metabol.2020.154414]

11 **Ahrén B**. Autonomic regulation of islet hormone secretion--implications for health and disease. *Diabetologia* 2000; **43**: 393-410 [PMID:

10819232 DOI: 10.1007/s001250051322]

12   **Salvioli B**, Bovara M, Barbara G, De Ponti F, Stanghellini V, Tonini M, Guerrini S, Cremon C, Degli Esposti M, Koumandou M, Corinaldesi R, Sternini C, De Giorgio R. Neurology and neuropathology of the pancreatic innervation. *JOP* 2002; **3**: 26-33 [PMID: 11884764]

13   **Thorens B**. Neural regulation of pancreatic islet cell mass and function. *Diabetes Obes Metab* 2014; **16** Suppl 1: 87-95 [PMID: 25200301 DOI: 10.1111/dom.12346]

14   **Hampton RF**, Jimenez-Gonzalez M, Stanley SA. Unravelling innervation of pancreatic islets. *Diabetologia* 2022; **65**: 1069-1084 [PMID: 35348820 DOI: 10.1007/s00125-022-05691-9]

15   **Giannulis I**, Mondini E, Cinti F, Frontini A, Murano I, Barazzoni R, Barbatelli G, Accili D, Cinti S. Increased density of inhibitory noradrenergic parenchymal nerve fibers in hypertrophic islets of Langerhans of obese mice. *Nutr Metab Cardiovasc Dis* 2014; **24**: 384-392 [PMID: 24462047 DOI: 10.1016/j.numecd.2013.09.006]

16   **Chiu YC**, Hua TE, Fu YY, Pasricha PJ, Tang SC. 3-D imaging and illustration of the perfusive mouse islet sympathetic innervation and its remodelling in injury. *Diabetologia* 2012; **55**: 3252-3261 [PMID: 22930160 DOI: 10.1007/s00125-012-2699-6]

17   **Masuo K**, Mikami H, Ogihara T, Tuck ML. Sympathetic nerve hyperactivity precedes hyperinsulinemia and blood pressure elevation in a young, nonobese Japanese population. *Am J Hypertens* 1997; **10**: 77-83 [PMID: 9008251 DOI: 10.1016/s0895-7061(96)00303-2]

18   **Lee DY**, Lee MY, Cho JH, Kwon H, Rhee EJ, Park CY, Oh KW, Lee WY, Park SW, Ryu S, Park SE. Decreased Vagal Activity and Deviation in Sympathetic Activity Precedes Development of Diabetes. *Diabetes Care* 2020; **43**: 1336-1343 [PMID: 32300048 DOI: 10.2337/dc19-1384]

19   **Manaka Y**, Watanabe M, Yamaguchi K, Manaka H, Kato T, Yamatani K, Tominaga M, Sasaki H. Sequential changes in CGRP-like immunoreactivity in NIDDM model Otsuka Long-Evans Tokushima Fatty (OLETF) rat pancreatic islets. *Pancreas* 1998; **17**: 72-79 [PMID: 9667523 DOI: 10.1097/00006676-199807000-00009]

20   **Martínez A**, Kapas S, Miller MJ, Ward Y, Cuttitta F. Coexpression of receptors for adrenomedullin, calcitonin gene-related peptide, and amylin in pancreatic beta-cells. *Endocrinology* 2000; **141**: 406-411 [PMID: 10614663 DOI: 10.1210/endo.141.1.7261]

21   **Moesgaard SG**, Brand CL, Sturis J, Ahrén B, Wilken M, Fleckner J, Carr RD, Svendsen O, Hansen AJ, Gram DX. Sensory nerve inactivation by resiniferatoxin improves insulin sensitivity in male obese Zucker rats. *Am J Physiol Endocrinol Metab* 2005; **288**: E1137-E1145 [PMID: 15883192 DOI: 10.1152/ajpendo.00356.2004]

22   **Brissova M**, Shostak A, Fligner CL, Revetta FL, Washington MK, Powers AC, Hull RL. Human Islets Have Fewer Blood Vessels than Mouse Islets and the Density of Islet Vascular Structures Is Increased in Type 2 Diabetes. *J Histochem Cytochem* 2015; **63**: 637-645 [PMID: 26216139 DOI: 10.1369/0022155415573324]

23   **Mukai E**, Ohta T, Kawamura H, Lee EY, Morita A, Sasase T, Miyajima K, Inagaki N, Iwanaga T, Miki T. Enhanced vascular endothelial growth factor signaling in islets contributes to β cell injury and consequential diabetes in spontaneously diabetic Torii rats. *Diabetes Res Clin Pract* 2014; **106**: 303-311 [PMID: 25262109 DOI: 10.1016/j.diabres.2014.08.023]

24   **Agudo J**, Ayuso E, Jimenez V, Casellas A, Mallol C, Salavert A, Tafuro S, Obach M, Ruzo A, Moya M, Pujol A, Bosch F. Vascular endothelial growth factor-mediated islet hypervascularization and inflammation contribute to progressive reduction of β-cell mass. *Diabetes* 2012; **61**: 2851-2861 [PMID: 22961079 DOI: 10.2337/db12-0134]

25   **de Sousa RAL**, de Lima EV, da Silva TP, de Souza RV, Figueiredo CP, Passos GF, Clarke JR. Late Cognitive Consequences of Gestational Diabetes to the Offspring, in a New Mouse Model. *Mol Neurobiol* 2019; **56**: 7754-7764 [PMID: 31115777 DOI: 10.1007/s12035-019-1624-0]

26   **Zhu Z**, Chen X, Xiao Y, Wen J, Chen J, Wang K, Chen G. Gestational diabetes mellitus alters DNA methylation profiles in pancreas of the offspring mice. *J Diabetes Complications* 2019; **33**: 15-22 [PMID: 30522793 DOI: 10.1016/j.jdiacomp.2018.11.002]

27   **Hokke SN**, Armitage JA, Puelles VG, Short KM, Jones L, Smyth IM, Bertram JF, Cullen-McEwen LA. Altered ureteric branching morphogenesis and nephron endowment in offspring of diabetic and insulin-treated pregnancy. *PLoS One* 2013; **8**: e58243 [PMID: 23516451 DOI: 10.1371/journal.pone.0058243]

28   **Piazza FV**, Segabinazi E, de Meireles ALF, Mega F, Spindler CF, Augustin OA, Salvalaggio GDS, Achaval M, Kruse MS, Coirini H, Marcuzzo S. Severe Uncontrolled Maternal Hyperglycemia Induces Microsomia and Neurodevelopment Delay Accompanied by Apoptosis, Cellular Survival, and Neuroinflammatory Deregulation in Rat Offspring Hippocampus. *Cell Mol Neurobiol* 2019; **39**: 401-414 [PMID: 30739252 DOI: 10.1007/s10571-019-00658-8]

29   **Kruse MS**, Barutta J, Vega MC, Coirini H. Down regulation of the proliferation and apoptotic pathways in the embryonic brain of diabetic rats. *Cell Mol Neurobiol* 2012; **32**: 1031-1037 [PMID: 22410672 DOI: 10.1007/s10571-012-9820-8]

30   **Munoz-Islas E**, Elizondo-Martinez CE, Gutierrez-Lopez M, Acosta-Gonzalez RI, Zaga-Clavellina V, Helguera-Repetto AC, Ramirez-Rosas MB, Romero-Sandoval EA, Jimenez-Andrade JM. Effect of Experimental Gestational Diabetes Mellitus on Mechanical Sensitivity, Capsaicin-Induced Pain Behaviors and Hind Paw Glabrous Skin Innervation of Male and Female Mouse Offspring. *J Pain Res* 2021; **14**: 1573-1585 [PMID: 34103982 DOI: 10.2147/JPR.S313467]

31   **Lindsay TH**, Halvorson KG, Peters CM, Ghilardi JR, Kuskowski MA, Wong GY, Mantyh PW. A quantitative analysis of the sensory and sympathetic innervation of the mouse pancreas. *Neuroscience* 2006; **137**: 1417-1426 [PMID: 16388907 DOI: 10.1016/j.neuroscience.2005.10.055]

32   **Alvarsson A**, Jimenez-Gonzalez M, Li R, Rosselot C, Tzavaras N, Wu Z, Stewart AF, Garcia-Ocaña A, Stanley SA. A 3D atlas of the dynamic and regional variation of pancreatic innervation in diabetes. *Sci Adv* 2020; **6** [PMID: 33036983 DOI: 10.1126/sciadv.aaz9124]

33   **Adamopoulos IE**, Wordsworth PB, Edwards JR, Ferguson DJ, Athanasou NA. Osteoclast differentiation and bone resorption in multicentric reticulohistiocytosis. *Hum Pathol* 2006; **37**: 1176-1185 [PMID: 16938523 DOI: 10.1016/j.humpath.2006.04.007]

34   **Koçer NE**, Kayaselçuk F, Calişkan K, Ulusan S. Synchronous GIST with osteoclast-like giant cells and a well-differentiated neuroendocrine tumor in Ampula Vateri: coexistence of two extremely rare entities. *Pathol Res Pract* 2007; **203**: 667-670 [PMID: 17656040 DOI: 10.1016/j.prp.2007.04.012]

35   **Lindsay TH**, Jonas BM, Sevcik MA, Kubota K, Halvorson KG, Ghilardi JR, Kuskowski MA, Stelow EB, Mukherjee P, Gendler SJ, Wong GY, Mantyh PW. Pancreatic cancer pain and its correlation with changes in tumor vasculature, macrophage infiltration, neuronal innervation, body weight and disease progression. *Pain* 2005; **119**: 233-246 [PMID: 16298491 DOI: 10.1016/j.pain.2005.10.019]

36   **Alvarsson A**, Jimenez-Gonzalez M, Li R, Rosselot C, Tzavaras N, Wu Z, Stanley SA. Optical Clearing and 3D Analysis Optimized for Mouse and Human Pancreata. *Bio Protoc* 2021; **11**: e4103 [PMID: 34458397 DOI: 10.21769/BioProtoc.4103]

37   **Zhang L**, Wang X, Wu Y, Lu X, Chidiac P, Wang G, Feng Q. Maternal diabetes up-regulates NOX2 and enhances myocardial ischaemia/reperfusion injury in adult offspring. *J Cell Mol Med* 2018; **22**: 2200-2209 [PMID: 29377505 DOI: 10.1111/jcmm.13500]

38   **Krishnaveni GV**, Hill JC, Leary SD, Veena SR, Saperia J, Saroja A, Karat SC, Fall CH. Anthropometry, glucose tolerance, and insulin

concentrations in Indian children: relationships to maternal glucose and insulin concentrations during pregnancy. *Diabetes Care* 2005; **28**: 2919-2925 [PMID: 16306555 DOI: 10.2337/diacare.28.12.2919]

39   **Yessoufou A**, Moutairou K. Maternal diabetes in pregnancy: early and long-term outcomes on the offspring and the concept of "metabolic memory". *Exp Diabetes Res* 2011; **2011**: 218598 [PMID: 22144985 DOI: 10.1155/2011/218598]

40   **Ding WG**, Guo LD, Kitasato H, Fujimura M, Kimura H. Phylogenic study of calcitonin gene-related peptide-immunoreactive structures in the pancreas. *Histochem Cell Biol* 1998; **109**: 103-109 [PMID: 9504770 DOI: 10.1007/s004180050207]

41   **Gram DX**, Ahrén B, Nagy I, Olsen UB, Brand CL, Sundler F, Tabanera R, Svendsen O, Carr RD, Santha P, Wierup N, Hansen AJ. Capsaicin-sensitive sensory fibers in the islets of Langerhans contribute to defective insulin secretion in Zucker diabetic rat, an animal model for some aspects of human type 2 diabetes. *Eur J Neurosci* 2007; **25**: 213-223 [PMID: 17241282 DOI: 10.1111/j.1460-9568.2006.05261.x]

42   **Canzano JS**, Nasif LH, Butterworth EA, Fu DA, Atkinson MA, Campbell-Thompson M. Islet Microvasculature Alterations With Loss of Beta-cells in Patients With Type 1 Diabetes. *J Histochem Cytochem* 2019; **67**: 41-52 [PMID: 29771178 DOI: 10.1369/0022155418778546]

43   **Willcox A**, Richardson SJ, Bone AJ, Foulis AK, Morgan NG. Analysis of islet inflammation in human type 1 diabetes. *Clin Exp Immunol* 2009; **155**: 173-181 [PMID: 19128359 DOI: 10.1111/j.1365-2249.2008.03860.x]

44   **Ehses JA**, Perren A, Eppler E, Ribaux P, Pospisilik JA, Maor-Cahn R, Gueripel X, Ellingsgaard H, Schneider MK, Biollaz G, Fontana A, Reinecke M, Homo-Delarche F, Donath MY. Increased number of islet-associated macrophages in type 2 diabetes. *Diabetes* 2007; **56**: 2356-2370 [PMID: 17579207 DOI: 10.2337/db06-1650]

45   **Steculorum SM**, Bouret SG. Maternal diabetes compromises the organization of hypothalamic feeding circuits and impairs leptin sensitivity in offspring. *Endocrinology* 2011; **152**: 4171-4179 [PMID: 21862611 DOI: 10.1210/en.2011-1279]

46   **Reynolds WA**, Chez RA, Bhuyan BK, Neil GL. Placental transfer of streptozotocin in the rhesus monkey. *Diabetes* 1974; **23**: 777-782 [PMID: 4278222 DOI: 10.2337/diab.23.9.777]

47   **Edwards RH**, Rutter WJ, Hanahan D. Directed expression of NGF to pancreatic beta cells in transgenic mice leads to selective hyperinnervation of the islets. *Cell* 1989; **58**: 161-170 [PMID: 2665941 DOI: 10.1016/0092-8674(89)90412-1]

48   **Bjerre B**, Björklund A, Mobley W, Rosengren E. Short- and long-term effects of nerve growth factor on the sympathetic nervous system in the adult mouse. *Brain Res* 1975; **94**: 263-277 [PMID: 1148872 DOI: 10.1016/0006-8993(75)90061-x]

49   **Kumar SD**, Yong SK, Dheen ST, Bay BH, Tay SS. Cardiac malformations are associated with altered expression of vascular endothelial growth factor and endothelial nitric oxide synthase genes in embryos of diabetic mice. *Exp Biol Med (Maywood)* 2008; **233**: 1421-1432 [PMID: 18824721 DOI: 10.3181/0806-RM-186]

50   **McDonald DM**, Choyke PL. Imaging of angiogenesis: from microscope to clinic. *Nat Med* 2003; **9**: 713-725 [PMID: 12778170 DOI: 10.1038/nm0603-713]